

Chemistry of the Phenoxathiins and  
Isosterically Related Heterocycles. XXXVII+.

The Synthesis and Molecular Structure of  
Benzo[2,3]naphtho[5,6,7-*ij*][1,4]dithiepin and its 1-Oxide

M. J. Musmar§, Saeed R. Khan, Andrew S. Zektzer# and Gary E. Martin\*‡

Department of Medicinal Chemistry, College of Pharmacy, University of Houston,  
Houston, Texas 77204-5515

Vincent M. Lynch and Stanley H. Simonsen\*

Department of Chemistry, The University of Texas at Austin,  
Austin, Texas 78512

Keith Smith\*

Department of Chemistry, University College of Swansea, Singleton Park,  
Swansea SA2 8PP, U.K.

Received June 10, 1988

Benzo[2,3]naphtho[5,6,7-*ij*][1,4]dithiepin was prepared by the condensation of the disodium salt of 1,2-dimercaptobenzene with 1-chloro-8-nitronaphthalene. The structure was established by nmr and mass spectroscopy. A small quantity of benzo[2,3]naphtho[5,6,7-*ij*][1,4]dithiepin 1-oxide was also isolated. The structure was initially established by mass spectrometry. The proton spectrum was totally assigned using a combination of proton zero quantum coherence (ZQCOSY) and proton-carbon heteronuclear chemical shift correlation (HC-COSY) techniques, which also allowed the unequivocal assignment of the protonated carbon resonances. An X-ray crystal structure of the 1-oxide irrefutably confirmed the structure. The crystal was triclinic and the space group was P1, and the data refined to a final R = 0.0353. The molecule was shown to be folded about the axis passing through the two sulfur atoms with a dihedral angle of 109.00°.

*J. Heterocyclic Chem.*, **26**, 667 (1989).

### Introduction.

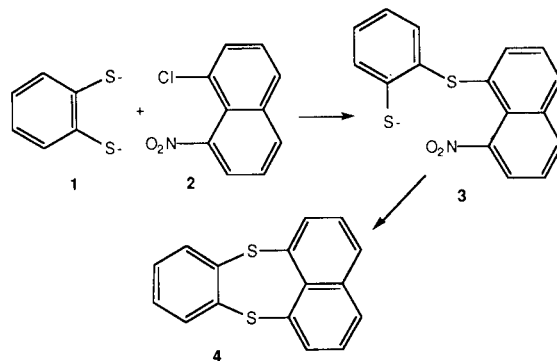
Recent efforts have led to the synthesis of both possible monoazathianthrenes [1,2] and the characterization of the parent 1-azathianthrene [3] and 4-nitro-2-azathianthrene [2] systems by X-ray crystallography. In addition, a number of di- and polyazathianthrenes have been prepared and studied crystallographically, including: 1,4-diazathianthrene [4]; benzo[*b*]-1,4-diazathianthrene [5]; 1,4,6,9-tetraazathianthrene [6]; and dibenzo[*b,i*]-1,4,6,9-tetraazathianthrene [7]. Interestingly, it appears from this limited group of compounds for which data are available that the folding of the azathianthrene analogs relative to the parent thianthrene system [3] occurs at the expense of the internal C-C-S bond angle of the 1,4-dithiin ring, the corresponding C-S-C angle remaining relatively constant. Thus, we were interested in examining the effect of increasing ring size from a 1,4-dithiin to 1,4-dithiepin. In particular, our interest was based upon the premise that the increased ring size would alleviate potential constraints imposed on the dihedral angle by the C-C-S bond angle, thereby possibly allowing the 1,4-dithiepin system to fold to an even greater extent than the parent thianthrene system. To test this hypothesis, the title compound, benzo[2,3]naphtho[5,6,7-*ij*][1,4]dithiepin and its mono *S*-oxide were studied.

### Results and Discussion.

Synthesis of Benzo[2,3]naphtho[5,6,7-*ij*][1,4]dithiepin (**4**).

The title compound, benzo[2,3]naphtho[5,6,7-*ij*][1,4]dithiepin (**4**) was prepared by the condensation of the dianion of 1,2-dimercaptobenzene (**1**) with 1-chloro-8-nitronaphthalene (**2**) in *N,N*-dimethylformamide as shown in Scheme I. It is presumed that the reaction proceeds *via* the initial displacement of the 1-chloro substituent to afford the thiophenolate sulfide intermediate **3** although this has not been confirmed. Preliminary identification of the reaction product (mp 142-144°, 45% isolated yield) as the desired 1,4-dithiepin analog, **4**, was provided by mass spectrometry, the compound exhibiting a molecular ion,  $M^+$ , at  $m/z = 266$  (100%) which was the base peak in the spectrum. Typical fragment ions were observed for the loss of S ( $m/z = 234$ , 60%), the loss of CS ( $m/z = 222$ , 8%) and the loss of CHS ( $m/z = 221$ , 7%). The proton nmr

Scheme I

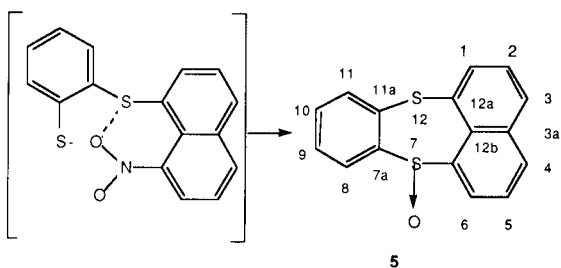


spectrum of **4** was intractable at 300 MHz, consisting of two complex, overlapped multiplets centered at approximately 7.20 ppm and 7.70 ppm with an integration ratio of 2:3, respectively.

#### Isolation and Identification of benzo[2,3]naphtho[5,6,7-*ij*][1,4]dithiepin 1-Oxide (**5**).

During a repeat synthesis, a small sample of material was isolated which exhibited a mp 194-195°. Mass spectrometry showed the molecular ion,  $M^+$ , to be  $m/z = 282$  (27%) with a fragment ion corresponding to loss of oxygen at  $m/z = 266$  (70%) which is consistent with the mass of the benzo[2,3]naphtho[5,6,7-*ij*][1,4]dithiepin (**4**) described above. Lower molecular weight fragment ions corresponded to the fragmentation pathway described for **4**. Based on this evidence, it was apparent that either during preparation or isolation that **4** had undergone an oxidation to afford the sulfoxide, benzo[2,3]naphtho[5,6,7-*ij*][1,4]dithiepin 1-oxide (**5**). Further evidence supportive of the sulfoxide structure was found in the 300 MHz proton nmr spectrum which showed resonances for ten non-equivalent protons. The analysis of the proton nmr spectrum is described in some detail below.

Two possible scenarios can be invoked to account for the structure of **5**. First, it is possible that the title compound, **4**, is susceptible to an extremely facile air oxidation. Alternatively, and perhaps more plausibly, it may be possible that an intramolecular transfer of oxygen from the nitro group to the sulfide linkage may occur prior to the closure of the 1,4-dithiepin ring by the second nucleophilic displacement. Support for this contention derives from the already reported observation of strong intramolecular sulfur-nitro group oxygen interactions by both  $^{13}\text{C}$ -nmr spectroscopy [8-11] and X-ray crystallographic techniques [10,12-15]. Regardless of how it was formed, the structure of benzo[2,3]naphtho[5,6,7-*ij*][1,4]dithiepin 1-oxide (**5**) is quite interesting and novel.



Eqn 1

#### Proton NMR Spectroscopy of Benzo[2,3]naphtho[5,6,7-*ij*][1,4]dithiepin 1-Oxide (**5**).

Congested proton nmr spectra of polynuclear aromatics can, in many cases, be intractable to analysis even by two-

dimensional nmr techniques such as autocorrelated proton (COSY) nmr. Recently, however, we have demonstrated the generally superior resolution afforded by proton zero quantum coherence (ZQCOSY) nmr experiments with a helicene analog, phenanthro[3',4':3,4]phenanthro[2,1-*b*]thiophene [16] and benzo[*b*]triphenylene[1,2-*d*]thiophene [17]. Furthermore, the ZQCOSY experiment is better suited to the establishment of vicinal proton connectivities than the COSY experiment. Thus, the proton ZQCOSY spectrum of **5** was acquired using the pulse sequence and phase cycling initially described by Müller [18] and utilized in our previous work [16,17].

The proton zero quantum spectrum of **5** optimized for an assumed 7 Hz vicinal coupling plotted at a fairly high contour level is shown in Figure 1. Only vicinal proton-proton connectivities are shown in the spectrum. Although the interpretation of ZQCOSY spectra has been treated in some detail in our earlier work [16], these experiments are still used rather infrequently and hence a reiteration on the interpretation of the spectra is in order. To begin, responses in the second or zero quantum frequency domain ( $F_1$ ) will appear at the algebraic difference of the offsets of the coupled spins relative to the transmitter. Referring to Figure 1, consider the 6/5 connectivity. Here, the doublet for H6 is observed to resonate approximately 185 Hz downfield of the position of the transmitter while the H5 resonance is centered about 20 Hz upfield of the transmitter position. Quite simply, the algebraic difference between the location of the two resonances is about 205 Hz and indeed, we note in the figure that sets of responses located at  $\pm 205$  Hz are correlated by a diagonal line with a slope of +2 which represents the 6/5 correlation pathway. Since the Müller [18] sequence provides quadrature detection in the second frequency domain *via* the 45° read pulse, the pair of responses which would normally be observed at ( $F_2 = +185$ ,  $F_1 = -205$ ) and ( $F_2 = -25$ ,  $F_1 = -205$ ) if a 90° read pulse were employed are totally suppressed. If present, the latter pair of responses would be correlated by an antidiagonal line with a slope of -2. It should also be noted for the interested reader that the splittings in the zero quantum frequency domain have recently been analyzed by Cavanagh and Keeler [19] and are currently being referred to as "K-splittings" in a sense analogous to the scalar coupling constant,  $J$ .

Beginning with the doublet resonating furthest downfield at 8.27 ppm in Figure 1, we may trace a connectivity network which ultimately comprises three spins (8.27, 7.60 and 7.84 ppm, H6, H5 and H4, respectively) which must hence be one of the three spin systems of the naphthyl portion of the molecule. Responses are located at the  $F_2$  frequency as in the normal one-dimensional spectrum and are displaced from the axis  $F_1 = 0$  Hz as a function of the

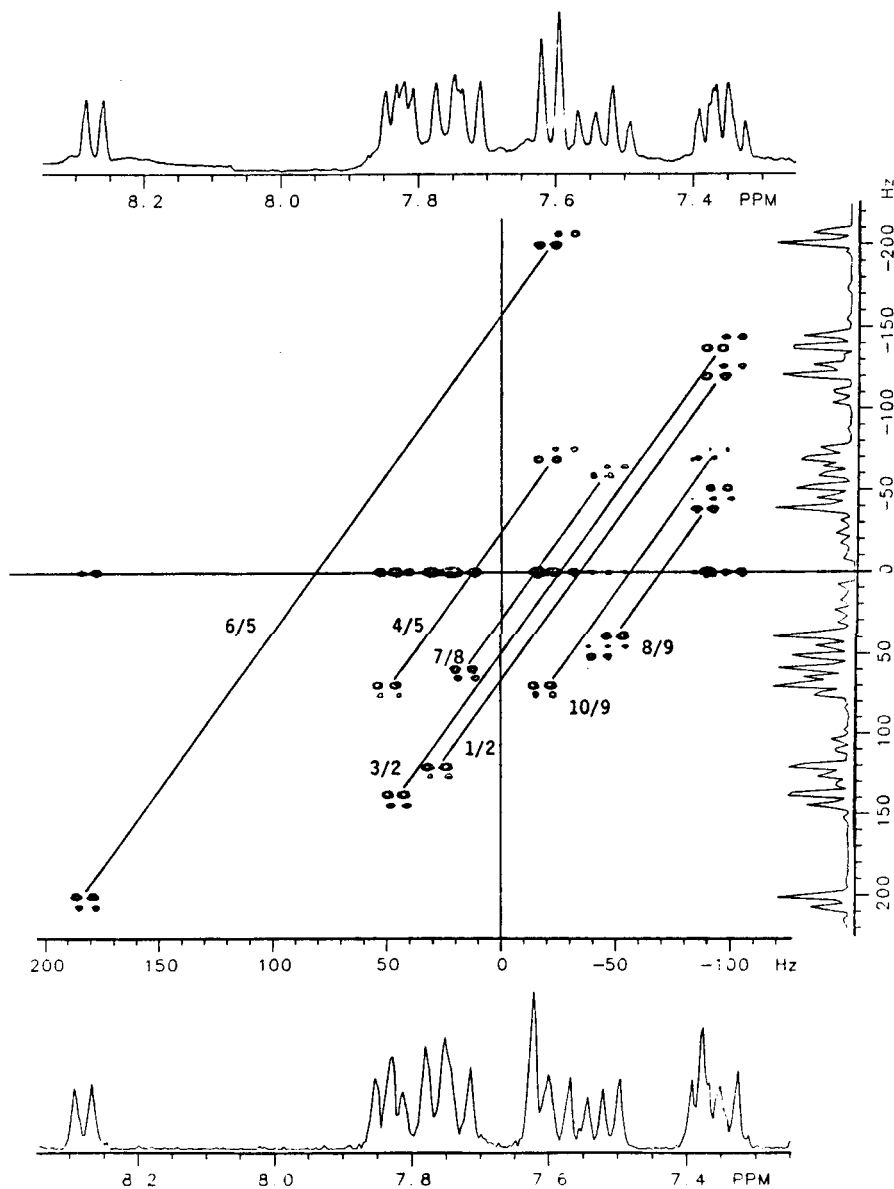


Figure 1. Proton zero quantum coherence two-dimensional nmr spectrum optimized for a 7 Hz (35.7 msec) vicinal coupling recorded using a sample of 10 mg of **5** recorded in deuteriochloroform at 300.068 MHz at an ambient probe temperature of 17°. The contour level plotted was chosen to show only vicinal proton-proton connectivities. A conventional high resolution proton spectrum is plotted below the contour plot. Chemical shifts in ppm are downfield of TMS. The axes flanking the contour plot in Hz are relative to the transmitter. The numbering scheme used in labelling the Figure is that shown in Table 1.

algebraic difference of the offsets of the coupled spins relative to the transmitter as described in detail above. Continuing from a resonance at 7.82 ppm which overlaps the resonance at 7.84 ppm to afford an apparent doublet of doublets in the one-dimensional spectrum, a second three spin system may be traced (7.82, 7.35 and 7.76 ppm, H10, H9 and H8, respectively) which constitutes the other three spins system of the naphthyl moiety. Finally, beginning at 7.76 ppm we may trace out the four spin system (7.72, 7.53,

7.37 and 7.84 ppm, H8, H9, H10 and H11, respectively) from the benzene derived portion of the molecular structure of **5**. In this fashion, the ZQCOSY spectrum shown in Figure 1 quite readily establishes the vicinal proton-proton connectivity network despite considerable congestion.

A much "deeper" contour plot of the ZQCOSY spectrum is shown in Figure 2 and establishes longer range intraring connectivities for which the experiment was not specifically optimized.

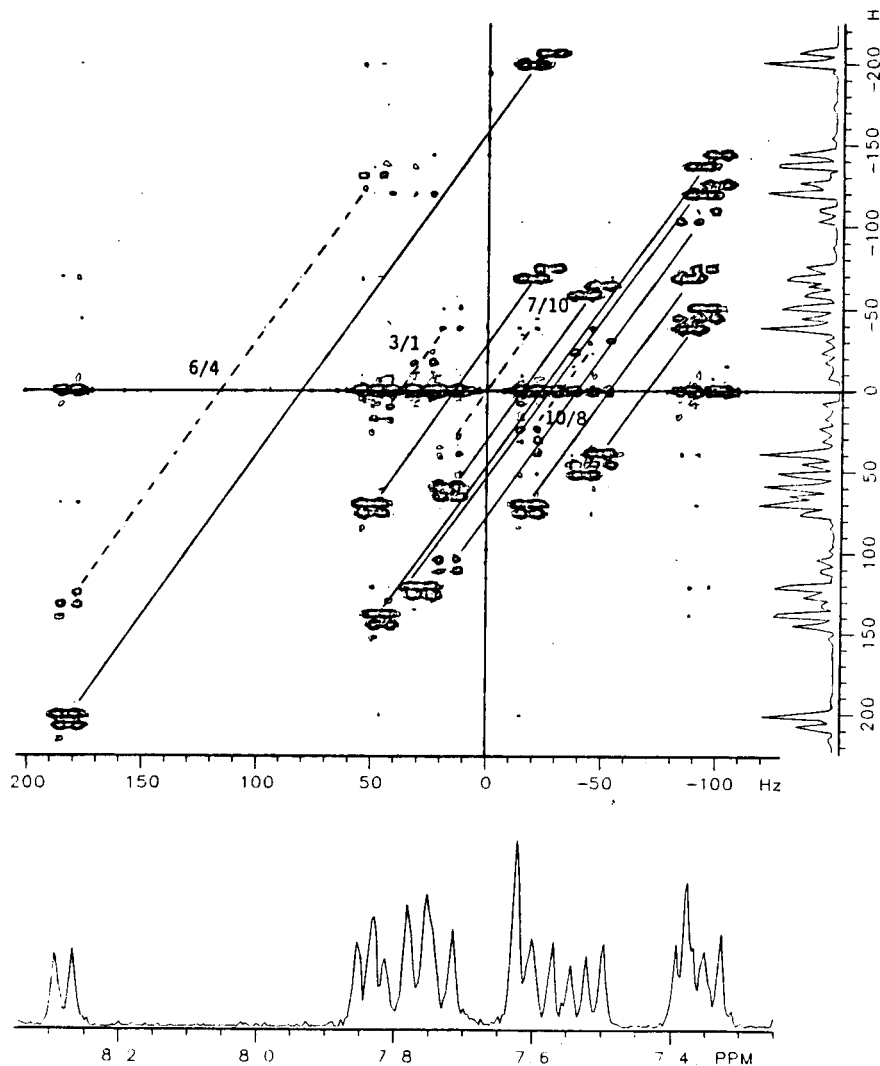


Figure 2. Proton zero quantum coherence two-dimensional nmr spectrum of **5** optimized for a 7 Hz vicinal coupling. The countour level plotted was chosen to show both vicinal proton-proton connectivities and the much weaker responses for longer range connectivities. A conventional high resolution proton spectrum is plotted below the contour plot. Chemical shifts in ppm are downfield of TMS. The axes flanking the contour plot in Hz are relative to the transmitter. The numbering scheme used in labeling the Figure is shown in Table 1.

Based upon the location of the two multiplets in the 300 MHz proton nmr spectrum of the parent compound, **4**, we have assigned the resonance furthest downfield as the H6 resonance (8.27 ppm). The assignments for H5 and H4 logically follow as 7.60 and 7.84 ppm, respectively. Since H3 would be expected to exhibit a similar chemical shift to H4, we have assigned the H3 resonance as 7.82 ppm. Careful examination of the region of the  $F_1 = 0$  Hz axis in the region from 7.82-7.84 ppm shows evidence for what may be a weak peri connectivity between the H3 and H4 resonances although this cannot be ascertained with complete certainty because of the axial response located at  $F_1 = 0$  Hz which arises due to longitudinal relaxation during the evolution period. The H2 and H1 resonances are then as-

signed as 7.35 and 7.76 ppm respectively.

With regard to the four spin system arising from the benzenoid portion of the molecule, we have assigned the H8 resonance at 7.72 ppm which is slightly downfield of the H11 resonance at 7.62 ppm. The H8 and H9 resonances are assigned as 7.53 and 7.37 ppm, respectively. Because of the minimal differences in the chemical shift of the H8 and H11 resonances, assignments based solely on proton chemical shift arguments may be considered to be reversible.

Carbon NMR Spectroscopy of Benzo[2,3]naphtho[5,6,7-*ij*]-[1,4]dithiepin 1-Oxide (**5**).

Potential ambiguities in the assignment of the proton

nmr spectrum of **5** may be resolved by considering the  $^{13}\text{C}$ -nmr spectrum of the compound. A proton-carbon heteronuclear chemical shift correlation spectrum (HC-COSY) with broadband homonuclear proton decoupling was acquired using the method described by Bax [20] and is shown in Figure 3. Direct heteronuclear correlations are quite obviously established by this method. Given the means of assigning one partner of a heteronuclear pair, the assignment of the other is unequivocally established.

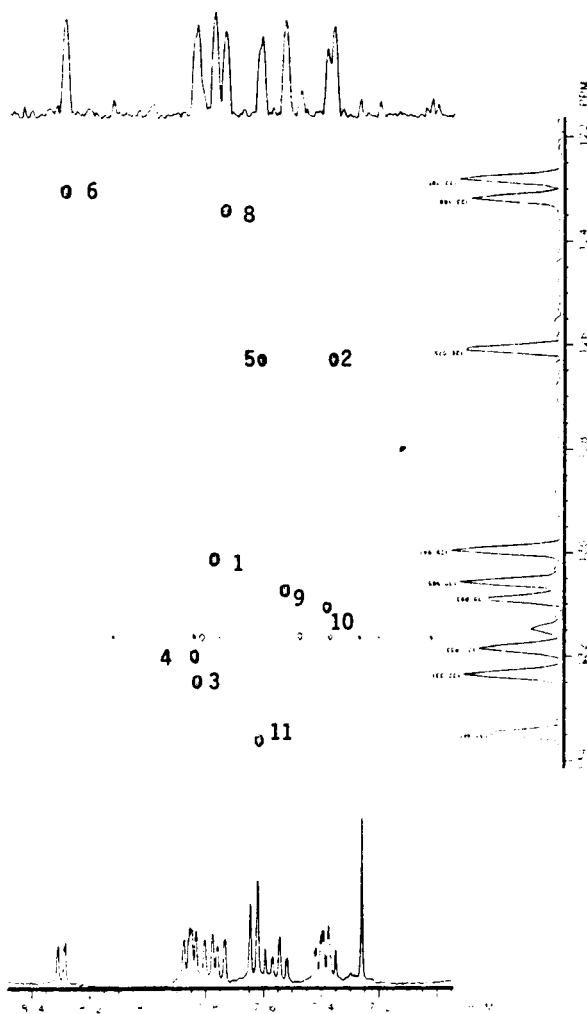


Figure 3. Proton-carbon heteronuclear chemical shift correlation spectrum with broadband homonuclear proton decoupling acquired using the pulse sequence and phase cycling of Bax [20].

Using chemical shift addivities derived from the work of Chauhan and Still [21] for the conversion of a thio-ether into its corresponding sulfoxide, we note that the positions ortho to a sulfoxide linkage are expected to be shifted upfield by 6.3 ppm relative to their unsubstituted counterparts. The meta position, in contrast would exhibit only a minimal downfield shift of about 0.1 ppm. Hence, we would expect the C6 and C8 resonances of **5** to be shifted upfield substantially relative to their C1 and C11 counter-

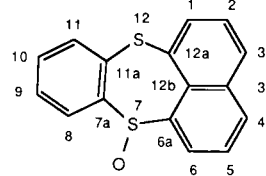
parts on the basis of additivity effects for the conversion of the sulfide to the sulfoxide.

It follows then from the tentative assignment of H6 as the resonance observed at 8.27 ppm, that C6 may be assigned as the carbon peak at 122.82 ppm. The C1 position, in contrast to C6, would be insulated from the chemical shift changes induced by sulfoxidation since it is in the other ring of the naphthyl portion of the molecule. Hence C1 would be expected to resonate downfield of C6 in the vicinity of approximately 129.1 ppm. From the proton tentatively assigned as H1 above (7.76 ppm) we note that the directly bonded carbon associated with the proton resonates at 129.96 ppm which is entirely consistent with the argument being developed. Finally, in close proximity to the now assigned chemical shift of C6, the carbon which may be assigned as C8 on the basis of the proton chemical shift of H8 suggested tentatively above is observed at 123.20 ppm.

The balance of the protonated carbon chemical shifts of **5** are collected in Table 1. An attempt was made to assign the quaternary carbon resonances of **5** using long range heteronuclear proton-carbon chemical shift correlation [22] but unequivocal assignments could not be made with the amount of material available for reasons of sensitivity. It is reasonably certain, however, on the basis of chemical shift considerations that the two quaternary carbons resonating furthest downfield (140.23 and 136.01 ppm) are attributable to the quaternary carbons bearing the sulfoxide sub-

Table 1

Proton and Protonated Carbon Chemical Shift Assignments of Benzo[2,3]naphtho[5,6,7-*ij*][1,4]dithiepin 1-Oxide (**5**) in Deuteriochloroform at 300.068 and 75.459 MHz for  $^1\text{H}$  and  $^{13}\text{C}$ , Respectively. [a]



| Position | $\delta^{\text{H}}$ (ppm) | $\delta^{\text{C}}$ (ppm) |
|----------|---------------------------|---------------------------|
| 1        | 7.76                      | 129.96                    |
| 2        | 7.35                      | 126.09                    |
| 3        | 7.82                      | 132.33                    |
| 4        | 7.84                      | 131.83                    |
| 5        | 7.60                      | 126.09                    |
| 6        | 8.27                      | 122.82                    |
| 7        | —                         | —                         |
| 8        | 7.72                      | 123.20                    |
| 9        | 7.53                      | 130.58                    |
| 10       | 7.37                      | 130.91                    |
| 11       | 7.62                      | 133.46                    |

[a] The numbering scheme for chemical shift data is that shown below.

stituent which are expected to be shifted downfield 9.9 ppm relative to their sulfide bearing counterparts [21]. For the four remaining quaternary carbon sites in the molecule, only three quaternary carbons were observed and these are unassigned. The missing carbon resonance is calculated to be accidentally overlapped by one of the protonated carbon resonances.

#### X-Ray Crystallography of Benzo[2,3]naphtho[5,6,7-*ij*][1,4]-dithiepin 1-Oxide.

A crystal of **5** suitable for X-ray crystallography was grown from chloroform. The atom labelling scheme used in the crystallographic study is shown in Figure 4 accompanied by bond distances; bond angles are shown in Figure 5. A view of the packing in the unit cell is shown in Figure 6 which clearly illustrates the non-planarity of **5**. Indeed, using the planes defined by the benzene ring and the naphthalene moiety, the dihedral angle about the sulfur/sulfoxide bond axis was  $111.29(4)^\circ$ . Including the sulfur atoms in the computation of the dihedral angle gives  $109.00(2)^\circ$ . Compound **5** is therefore substantially more folded than any of the thianthrene systems yet studied [2-7]. The C-C-S bond angles on the "benzene side" of the molecule are also smaller than in any of the thianthrene systems studied.

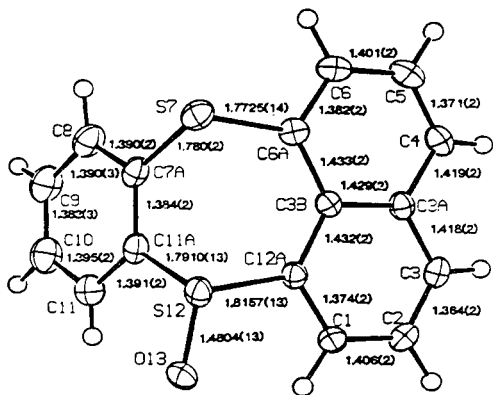


Figure 4. Atom labeling scheme for the x-ray crystallographic study of **5** which also shows bond distances.

A summary of the crystallographic data is given in the experimental section below. Positional and thermal parameters are contained in Table 2; torsional angles for the non-hydrogen atoms of **5** are given in Table 3. Least squares planes and dihedral angles for **5** are contained in Table 4. The S---S intramolecular distance was  $3.0594 \text{ \AA}$ , and is slightly smaller than the  $3.1926 \text{ \AA}$  distance found in the case of thianthrene [3] which may impose some constraint on the central ring.

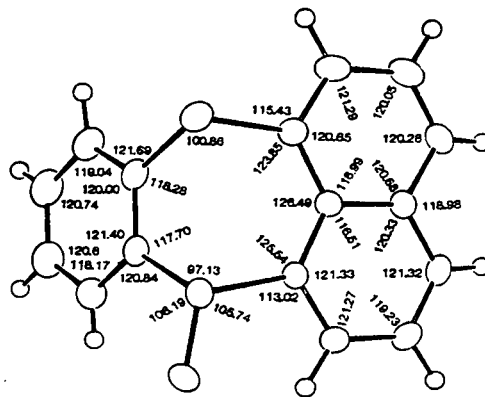


Figure 5. View of the structure of **5** showing bond angles for the non-hydrogen atoms.

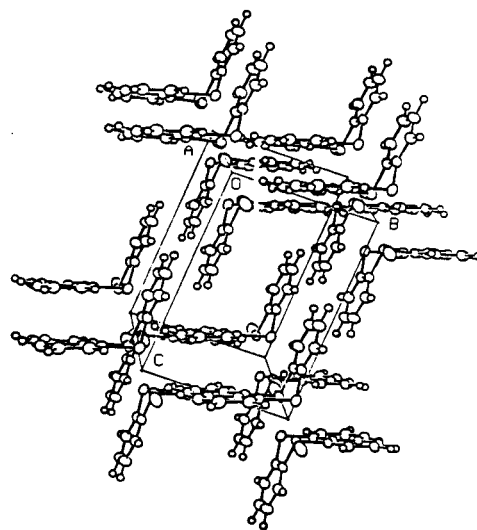


Figure 6. View of the unit cell of **5** showing the packing of the molecules in the crystal lattice and the folding of the molecule about the S7---S12 axis.

#### Conclusions.

Based on the observations just presented, it is logical to conclude that the increase in ring size afforded by the 1,4-dithiepin nucleus accommodates an increasing folding of the molecule about the S---S axis thereby accounting for the dihedral angle of  $109.0^\circ$  for **5**, which is in sharp contrast to the  $127.14^\circ$  dihedral angle observed for the parent thianthrene [3].

The mechanism responsible for the formation of **5** remains to be confirmed. It is quite possible, however, that the formation of **5** occurs during the synthesis of **4** as a competing reaction, with intramolecular transfer of the oxygen atom from the nitro group to the sulfur as shown in Equation 1.

Table 2

Positional and Thermal Parameters for Benzo[2,3]naphtho[5,6,7-*ij*][1,4]-dithiepin 1-Oxide (5) [a]

| Atom | x         | y         | z          | u          |
|------|-----------|-----------|------------|------------|
| C1   | .2485(2)  | .5274(2)  | .09074(12) | .0231(4)   |
| C2   | .2956(2)  | .7063(2)  | .06579(12) | .0253(4)   |
| C3   | .4793(2)  | .7965(2)  | .09320(12) | .0240(4)   |
| C3a  | .6234(2)  | .7136(2)  | .14675(11) | .0205(4)   |
| C3b  | .5785(2)  | .5326(2)  | .17437(11) | .0187(3)   |
| C4   | .8124(2)  | .8124(2)  | .17089(13) | .0256(4)   |
| C5   | .9457(2)  | .7357(2)  | .22264(14) | .0297(4)   |
| C6   | .9140(2)  | .5606(2)  | .25431(13) | .0269(4)   |
| C6a  | .7318(2)  | .4601(2)  | .23173(11) | .0216(4)   |
| S7   | .70552(5) | .23787(4) | .27122(3)  | .02642(12) |
| C7a  | .5627(2)  | .2376(2)  | .37246(12) | .0242(4)   |
| C8   | .6343(2)  | .2429(2)  | .49808(13) | .0313(5)   |
| C9   | .5149(3)  | .2382(2)  | .57221(14) | .0370(5)   |
| C10  | .3271(3)  | .2269(2)  | .52222(15) | .0368(5)   |
| C11  | .2535(2)  | .2198(2)  | .39622(14) | .0306(5)   |
| C11a | .3745(2)  | .2260(2)  | .32286(12) | .0234(4)   |
| S12  | .28932(4) | .20938(4) | .15991(3)  | .02361(11) |
| C12a | .3840(2)  | .4427(2)  | .14371(11) | .0191(3)   |
| O13  | .0845(2)  | .1848(2)  | .13221(11) | .0323(4)   |
| O13a | .861(2)   | .212(2)   | .3553(12)  | .050(3)    |
| H1   | .118(3)   | .457(3)   | .077(2)    | .059(7)    |
| H2   | .199(3)   | .772(3)   | .028(2)    | .036(5)    |
| H3   | .517(3)   | .915(3)   | .079(2)    | .047(6)    |
| H4   | .836(3)   | .931(3)   | .154(2)    | .034(5)    |
| H5   | 1.083(3)  | .806(3)   | .239(2)    | .044(5)    |
| H6   | 1.016(3)  | .499(3)   | .292(2)    | .045(5)    |
| H8   | .762(3)   | .234(3)   | .531(2)    | .035(5)    |
| H9   | .558(3)   | .244(3)   | .658(2)    | .042(5)    |
| H10  | .240(3)   | .231(3)   | .581(2)    | .056(6)    |
| H11  | .138(3)   | .223(3)   | .368(2)    | .049(6)    |

[a] The numbering scheme for the crystallographic data is that shown in Figure 4.

Table 3

Torsion Angles for the Non-hydrogen Atoms of Benzo[2,3]naphtho[5,6,7-*ij*][1,4]dithiepin 1-Oxide (5) [a]

| 1    | 2  | 3    | 4   | 1-2-3-4     |
|------|----|------|-----|-------------|
| C2   | C1 | C12a | C3b | -.7(2)      |
| C2   | C1 | C12a | S12 | -177.20(11) |
| C12a | C1 | C2   | C3  | .9(2)       |
| C1   | C2 | C3   | C3a | -.3(2)      |
| C2   | C3 | C3a  | C3b | -.6(2)      |

|      |      |      |      |             |
|------|------|------|------|-------------|
| C2   | C3   | C3a  | C4   | 178.61(14)  |
| C3b  | C3a  | C4   | C5   | -.8(2)      |
| C4   | C3a  | C3b  | C6a  | 2.7(2)      |
| C4   | C3a  | C3b  | C12a | -178.41(12) |
| C3   | C3a  | C3b  | C6a  | -178.19(12) |
| C3   | C3a  | C3b  | C12a | .7(2)       |
| C3   | C3a  | C4   | C5   | 179.98(14)  |
| C6a  | C3b  | C12a | C1   | 178.70(13)  |
| C6a  | C3b  | C12a | S12  | -5.3(2)     |
| C12a | C3b  | C6a  | C6   | 178.79(13)  |
| C12a | C3b  | C6a  | S7   | 2.1(2)      |
| C3a  | C3b  | C6a  | C6   | -2.4(2)     |
| C3a  | C3b  | C6a  | S7   | -179.09(10) |
| C3a  | C3b  | C12a | C1   | -.1(2)      |
| C3a  | C3b  | C12a | S12  | 175.89(10)  |
| C3a  | C4   | C5   | C6   | -1.3(2)     |
| C4   | C5   | C6   | C6a  | 1.6(2)      |
| C5   | C6   | C6a  | C3b  | .3(2)       |
| C5   | C6   | C6a  | S7   | 177.28(12)  |
| C3b  | C6a  | S7   | C7a  | -59.30(12)  |
| C3b  | C6a  | S7   | O13a | -162.34(7)  |
| C6   | C6a  | S7   | C7a  | 123.85(11)  |
| C6   | C6a  | S7   | O13a | 20.8(7)     |
| O13a | S7   | C7a  | C8   | 10.1(6)     |
| O13a | S7   | C7a  | C11a | -167.8(5)   |
| C6a  | S7   | C7a  | C8   | -105.94(12) |
| C6a  | S7   | C7a  | C11a | 76.14(11)   |
| C8   | C7a  | C11a | C11  | .2(2)       |
| C8   | C7a  | C11a | S12  | -177.19(11) |
| C11a | C7a  | C8   | C9   | -.7(2)      |
| S7   | C7a  | C8   | C9   | -178.54(12) |
| S7   | C7a  | C11a | C11  | 178.11(11)  |
| S7   | C7a  | C11a | S12  | .76(14)     |
| C7a  | C8   | C9   | C10  | .6(2)       |
| C8   | C9   | C10  | C11  | .0(3)       |
| C9   | C10  | C11  | C11a | -.5(2)      |
| C10  | C11  | C11a | C7a  | .4(2)       |
| C10  | C11  | C11a | S12  | 177.70(12)  |
| C7a  | C11a | S12  | C12a | -75.59(11)  |
| C7a  | C11a | S12  | O13  | 175.68(10)  |
| C11  | C11a | S12  | C12a | 107.05(12)  |
| C11  | C11a | S12  | O13  | -1.68(13)   |
| O13  | S12  | C12a | C1   | -10.79(12)  |
| O13  | S12  | C12a | C3b  | 172.91(11)  |
| C11a | S12  | C12a | C1   | -119.89(11) |
| C11a | S12  | C12a | C3b  | 63.81(13)   |

[a] Atoms are labeled for the crystallographic study using the numbering scheme shown in Figure 4.

Table 4

Least Squares Planes and Dihedral Angles for Benzo[2,3]naphtho-  
[5,6,7-*ij*][1,4]dithiepin 1-Oxide (5) [a]

|  |           |       |           |
|--|-----------|-------|-----------|
| Equation for Plane 1                             |           |       |           |
| $-3.13253x + 2.60376y + 12.32026z - 1.71888 = 0$ |           |       |           |
| C1   | .006(2)   | C2    | -.005(2)  |
| C3a  | .006(2)   | C3b   | -.004(2)  |
| S12*   | .1099(7)  | C4*   | .043(2)   |
| C6   | -.011(2)  | C6a*  | -.042(2)  |
| C3   | -.002(2)  | C12a  | -.002(2)  |
| C5*  | .051(2)   | S7*   | -.0319(8) |
| $\chi^2 = 47.68$                                 |           |       |           |
| Equation for Plane 2                             |           |       |           |
| $3.06983x - 2.78701y - 12.20012z + 1.85264 = 0$  |           |       |           |
| C3a  | -.013(2)  | C3b   | .017(2)   |
| C5   | .017(2)   | C6    | -.006(2)  |
| C1*  | .039(2)   | C2*   | -.011(2)  |
| S7*  | .0466(8)  | C12a* | .044(2)   |
| C4   | -.002(2)  | C6a   | -.010(2)  |
| C3*  | -.033(2)  | S12*  | .2064(8)  |
| $\chi^2 = 349.66$                                |           |       |           |
| Equation for Plane 3                             |           |       |           |
| $3.10572x - 2.69723y - 12.25954z + 1.78056 = 0$  |           |       |           |
| C1   | -.018(2)  | C2    | .013(2)   |
| C3a  | .007(2)   | C3b   | -.003(2)  |
| C5   | -.032(2)  | C6    | .010(2)   |
| C12a   | -.017(2)  | S7*   | -.0051(7) |
| C3   | .022(2)   | C4    | -.018(2)  |
| C6a  | .029(2)   | S12*  | -.1540(6) |
| $\chi^2 = 1295.83$                               |           |       |           |
| Equation for Plane 4                             |           |       |           |
| $3.36781x - 2.57919y - 12.28609z + 1.55068 = 0$  |           |       |           |
| C1   | .087(2)   | C2    | .084(2)   |
| C3a  | -.007(2)  | C3b   | .017(1)   |
| C5   | -.133(2)  | C6    | -.059(2)  |
| C12a   | .064(1)   | S7    | .190(5)   |
| C3   | .035(2)   | C4    | -.092(2)  |
| C6a  | .019(2)   | S12   | -.0204(4) |
| $\chi^2 = 44209.61$                              |           |       |           |
| Equation for Plane 5                             |           |       |           |
| $0.42573x - 7.56080y + 0.123617z + 1.50880 = 0$  |           |       |           |
| C7a  | .002(1)   | C8    | -.004(2)  |
| C10  | .003(2)   | C11   | -.004(2)  |
| S7*  | -.0442(7) | S12*  | -.0687(7) |
| C9   | .002(2)   | C11a  | .001(1)   |
| $\chi^2 = 19.89$                                 |           |       |           |
| Equation for Plane 6                             |           |       |           |
| $-0.42144x + 7.57064y - 0.35194z - 1.40840 = 0$  |           |       |           |
| C7a  | .022(1)   | C8    | -.012(2)  |
| C10  | -.013(2)  | C11   | .010(2)   |
| S7   | -.0004(4) | S12   | -.0015(3) |
| C9   | -.023(2)  | C11a  | .031(1)   |

 $\chi^2 = 9734.30$ 

Dihedral Angles Between Selected Planes

|   |   |            |
|---|---|------------|
| 1 | 2 | 1.60(4)°   |
| 3 | 5 | 111.29(4)° |
| 4 | 6 | 109.00(2)° |

[a] All distances are given in angstroms from the plane. Atoms denoted by \* were not used in the plane calculation. The numbering scheme used in this table is shown in Figure 4.

## EXPERIMENTAL

Melting points were determined in open capillary tubes in a Thomas-Hoover apparatus and are reported uncorrected. Elemental analyses were performed by Atlantic Microlabs, Atlanta, GA. All infrared spectra were obtained using a Perkin Elmer model 283 spectrophotometer as 1% potassium bromide pellets.

Synthesis of Benzo[2,3]naphtho[5,6,7-*ij*][1,4]dithiepin (4).

To a 100 ml three neck flask was added 0.13 g (0.0054 mole) of sodium hydride in 50 ml of dry, freshly distilled *N,N*-dimethylformamide (DMF) and 0.35 g (0.0024 mole) of 1,2-dimercaptobenzene (Fluka) under an inert argon atmosphere. The suspension was stirred until hydrogen evolution ceased (about 2 hours) after which the flask was cooled in an ice bath. Next, 0.35 g (0.00168 mole) of 1-chloro-8-nitronaphthalene was added and the flask stirred for a further 2 hours prior to the initiation of reflux, which was continued for 8 hours. After cooling, the reaction mixture was poured into 250 ml of ice cold distilled water which was extracted with 4 × 100 ml portions of ethyl acetate. The combined ethyl acetate extracts were then back extracted with 2 × 100 ml of distilled water after which the ethyl acetate solution was dried over anhydrous sodium sulfate. On concentration, 0.25 g (45% yield) of a white crystalline material (mp 142-144°) was isolated by filtration. The infrared spectrum of the isolated material gave:  $\lambda$  (cm<sup>-1</sup>) 1750, 1625, 1535, 1350, 870, 830. The electron impact low resolution mass spectrum of 4 gave: *m/z* (% relative intensity) 266 (M<sup>+</sup>, 100), 268 (M<sup>+</sup> + 2, 9), 234 (M<sup>+</sup> - S, 60), 222 (M<sup>+</sup> - CS, 8), 221 (M<sup>+</sup> - CHS, 7). The 300 MHz <sup>1</sup>H-nmr spectrum is discussed in the text. The <sup>13</sup>C resonances observed at 75 MHz in deuteriochloroform: protonated carbon resonances - 125.72, 129.45, 130.31, 132.23, 132.85  $\delta$ ; quaternary carbon resonances - 133.14, 136.61, 142.37  $\delta$ .

Anal. Calcd. for C<sub>16</sub>H<sub>10</sub>S<sub>2</sub>: C, 72.18; H, 3.75; S, 24.06. Found: C, 71.95; H, 3.81; S, 23.91.

Isolation of Benzo[2,3]naphtho[5,6,7-*ij*][1,4]dithiepin 1-Oxide (5).

During a subsequent preparation of the parent dithiepin, 4, a small quantity of a light brown compound (23 mg) mp 194-195° was isolated. The low resolution electron impact mass spectrum of the compound gave a molecular ion, M<sup>+</sup>, at *m/z* = 282 (27%). An intense fragment ion was observed at *m/z* = 266 (70%) corresponding to 4. Lower mass fragment ions were consistent with the fragmentation described for 4 above. On this basis, the compound was tentatively identified as benzo[2,3]naphtho[5,6,7-*ij*][1,4]dithiepin 1-oxide (5). The structure of the molecule was confirmed by two-dimensional nmr methods using 10 mg of material recrystallized from chloroform. Slow evaporation of the deuteriochloroform from the tightly capped nmr tube gave a crystal suitable for X-ray crystallography. Losses during purification precluded elemental analysis.

NMR Spectroscopy.

All nmr spectra were recorded using a Nicolet NT-300 wide bore spectrometer operating at frequencies of 300.068 and 75.459 MHz for <sup>1</sup>H and <sup>13</sup>C observation, respectively. The instrument was controlled by a model 293-C pulse programmer and was equipped with a 5 mm <sup>1</sup>H/<sup>13</sup>C dual tuned probe. Typical instrument parameters were: 60° tip for one dimen-



sional experiments = 10.0  $\mu\text{sec}$  for  $^1\text{H}$  and 11.6  $\mu\text{sec}$  for  $^{13}\text{C}$ ; 1 sec interpulse delay; sweep widths were  $\pm 2$  KHz for  $^1\text{H}$  and  $\pm 9.6$  KHz for  $^{13}\text{C}$ ; proton spectra were digitized with 16K complex points,  $^{13}\text{C}$  spectra were digitized with 32K complex points; all data were taken using quadrature phase detection. Chemical shifts are reported in ppm downfield from TMS. All spectra were acquired at an ambient probe temperature of 17°.

The two-dimensional proton zero quantum coherence experiment (ZQCOSY performed on **5** employed a sample of 10 mg of **5** in 0.4 ml of deuteriochloroform and used the pulse sequence described by Müller [18] with a 64 step phase cycle as reported in our previous work [16]. The data was acquired as  $470 \times 2\text{K}$  complex points overnight with a sweep width in  $F_2 = \pm 243$  Hz. The incremented evolution time in  $F_1$  was set to 0.5° dwell in  $F_2 = 1$  msec. A 45° reconversion pulse was employed to convert the evolved zero quantum coherence back into observable single quantum coherence prior to acquisition. The data was processed using sinusoidal multiplication prior to both Fourier transformations with zero filling to 512 points prior to the second. Data is shown in Figures 1 and 2.

The proton-carbon heteronuclear two-dimensional chemical shift correlation spectrum with broadband homonuclear proton decoupling shown in Figure 3 was recorded using the pulse sequence and phase cycling described by Bax [20]. The experiment was performed using the same sample as for the proton zero quantum experiment described above. Data was acquired overnight as  $90 \times 1\text{K}$  complex points using a 1 sec interpulse delay. Spectral widths were  $F_1 = \pm 243$  Hz and  $F_2 = \pm 2100$  Hz. The data was processed using a 2 Hz exponential broadening prior to the first Fourier transformation and a double exponential apodization and zero filling to 256 points prior to the second Fourier transformation. The data is shown in Figure 3.

An attempt was made to record the long range heteronuclear chemical shift correlation spectrum of **5** using the pulse sequence modified to provide one bond modulation decoupling recently described by Zektzer, John and Martin [22]. Although some responses were observed after processing of the data from a 40 hour accumulation, the signal to noise ratio in the spectrum was insufficient to allow the unequivocal assignment of any of the quaternary carbon resonances.

#### X-Ray Crystallography.

A nearly colorless block measuring .40 mm  $\times$  .33 mm  $\times$  .37 mm was obtained from the slow evaporation of deuteriochloroform from a tightly capped 5 mm nmr tube. A Syntex P2, diffractometer was used for the X-ray crystallographic study and was equipped with a graphite monochromator, Mo K $\alpha$  radiation ( $\lambda = 0.71069 \text{ \AA}$ ) and a Syntex LT-1 low temperature delivery system (163°K). Lattice parameters were determined from least squares refinement of 60 reflections with  $25.1^\circ < 2\theta < 30.9^\circ$ . The crystal system is triclinic, space group is P1. Lattice constants:  $a = 7.642(2)$ ,  $b = 7.709(2)$ ,  $c = 11.395(2) \text{ \AA}$ ,  $\alpha = 92.77(1)$ ,  $\beta = 104.84(1)$ ,  $\gamma = 103.24(1)^\circ$ ,  $V = 627.6(3) \text{ \AA}^3$ ,  $Z = 2$ ,  $d_x = 1.49 \text{ g-cm}^{-3}$ ,  $F(000) = 292$ . The omega scan technique (3649 reflections) was used;  $2\theta$  range  $4-60^\circ$ ,  $1^\circ \omega$  scan at  $3-6^\circ \text{ min}^{-1}$ . ( $h = -10-10$ ,  $k = -10-10$ ,  $l = -15-16$ ). Four reflections (0,0,4; -3,0,0; 0,5,0; 1,2,2) were remeasured every 96 reflections to monitor instrument and crystal stability. No evidence of crystal decay was noted. Data corrected for Lp effects and absorption (based on crystal shape,  $\mu = 3.93 \text{ cm}^{-1}$ ; transmission factor range 0.866-0.890). Data reduction was performed as described by Riley and Davis [23]. Reflections have  $F_o < 4\sigma(F_o)$  were considered unobserved (303 reflections). The structure was solved by MULTAN78 [24] and was refined by full-matrix least squares procedures [25] with anisotropic thermal parameters for non-hydrogen atoms. Hydrogen atoms were located from a Fourier difference map and were refined with isotropic thermal parameters; 216 parameters were refined. The function  $\Sigma w(|F_o| - |F_c|)^2$  was minimized where  $w = 1/(\sigma(F_o))^2$  and  $\sigma(F_o) = .5kI^{-1/2}(\sigma(I))^2 + (.04I)^{1/2}$ . Intensity,  $I$ , given by  $(I_{\text{peak}} - I_{\text{background}}) \times (\text{scan rate})$ . 0.04 is a factor to downweight intense reflections and to account for instrument stability and  $k$  is the correction due to Lp effects and absorption. Sigma(I) estimated from counting statistics;  $\sigma(I) = [(I_{\text{peak}} - I_{\text{background}})]^{1/2} \times (\text{scan rate})$ . Final  $R = .0353$  for 3346 reflections,  $wR = .0532$  ( $R_{\text{int}} = .0384$ ,  $wR_{\text{int}} = .0552$ ) and a goodness of fit = 2.12. Maximum  $|\Delta f/\sigma| < 0.1$  in the final refinement cy-

cle and the minimum and maximum peaks in the  $\Delta F$  map were  $-0.20$  and  $0.57 \text{ e}^{-1} \text{ \AA}^3$ , respectively. After several cycles of refinement with all H atoms input, a large peak ( $1.2 \text{ e}^{-1} \text{ \AA}^3$ ) persisted  $1.42 \text{ \AA}$  from S7, close to the expected S-O bond length in a sulfoxide. The electron density associated with this peak could not account for an oxygen atom at full occupancy and it was therefore concluded that the oxygen atom was disordered about two positions near S12. The occupancy factors for the oxygen atom were refined to 89.6(3)% for O13 and 10.4(3)% for O13a. O13a was refined isotropically. The disorder of the oxygen atom required that the sulfur atoms also be disordered since the geometry around a sulfide sulfur atom is different from that around a sulfoxide sulfur atom. However attempts to split the sulfur atoms into two separate atoms representing a sulfoxide sulfur and a sulfide sulfur resulted in the merging of the two peaks into a single peak on refinement. No evidence of disorder was observed in the carbon atom positions. Scattering factors for the non-hydrogen atoms were taken from Cromer and Mann [26], while scattering factors for the hydrogen atoms were from Stewart, Davidson and Simpson [27]; linear absorption coefficients were taken from the International Tables for X-ray Crystallography [28]. The least squares planes program was supplied by Cordes [29]; other computer programs are cited in reference 11 of Gadol and Davis [30].

#### Acknowledgements.

The authors would like to thank the Robert A. Welch Foundation for its support of this work through Grants No. E-792 and F-017 to G. E. M. and S. H. S. the former providing a predoctoral fellowship for S. R. K. and a postdoctoral fellowship for A. S. Z., G. E. M. and K. S. also wish to thank the North Atlantic Treaty Organization for support through Grant No. 019.81. Finally, the support of the University of Houston, which provided partial funding for the acquisition of the NT-300 spectrometer used in this research is also acknowledged as is the ongoing technical assistance of Mr. L. D. Sims.

#### REFERENCES AND NOTES

- + This paper also represents Part **33** in the Series Novel Heterocyclic Compounds. For the preceding paper in that series, see: K. Smith, C. M. Lindsay and I. K. Morris, "Convenient Syntheses of 4-Aminopyridine-3-thiol and Several Thiazolo[5,4-c]pyridines", in preparation. For the previous paper in the series Chemistry of the Phenoxathiins, see: the paper cited in ref [11] of this work.
- \* To whom inquiries should be addressed.
- § Present address: Department of Chemistry, University of South Florida, Tampa, Florida 33620.
- # Present address: Abbott Laboratories, Abbott Park, Illinois, 60064.
- ‡ Present Address: Burroughs Wellcome Co., Wellcome Research Laboratories, 3030 Cornwallis Rd., Research Triangle Park, NC 27709.
- [1] S. Puig-Torres, G. E. Martin, J. J. Ford, M. R. Willcott, III and K. Smith, *J. Heterocyclic Chem.*, **19**, 1441 (1982).
- [2] W. W. Lam, G. E. Martin, V. M. Lynch, S. H. Simonsen, C. M. Lindsay and K. Smith, *ibid.*, **23**, 747 (1986).
- [3] S. B. Larson, S. H. Simonsen, G. E. Martin, K. Smith, S. Puig-Torres, *Acta Cryst.*, **C40**, 103 (1983).
- [4] S. B. Larson, S. H. Simonsen, W. W. Lam, G. E. Martin, C. M. Lindsay and K. Smith, *ibid.*, **C41**, 1781 (1985).
- [5] C. M. Lindsay, K. Smith, W. W. Lam, M. J. Musmar, G. E. Martin, A. F. Hoffschwele, V. M. Lynch and S. H. Simonsen, manuscript in preparation.
- [6] W. W. Lam, M. J. Musmar, G. E. Martin, K. Smith, V. M. Lynch and S. H. Simonsen, unpublished data.
- [7] A. Pignedoli, G. Peyranel and L. Antorini, *J. Cryst. Mol. Struct.*, **7**, 173 (1977).
- [8] G. E. Martin and J. C. Turley, *J. Heterocyclic Chem.*, **15**, 609 (1978).
- [9] J. C. Turley and G. E. Martin, *ibid.*, **18**, 431 (1981).
- [10] M. Kimura, S. H. Simonsen, S. R. Caldwell and G. E. Martin, *ibid.*, **18**, 469 (1981).

- [11] M. U. Mehta, G. E. Martin and K. Smith, *ibid.*, **24**, 235 (1987).  
[12] J. L. Ricci and I. Bernal, *J. Chem. Soc.*, 806 (1970).  
[13] J. D. Korp, I. Bernal, R. F. Miller, J. C. Turley, L. Williams and G. E. Martin, *J. Cryst. Molec. Struct.*, **8**, 127 (1978).  
[14] M. B. Hossain, C. A. Dwiggin, D. van der Helm, P. K. Sen Gupta, J. C. Turley and G. E. Martin, *Acta Cryst.*, **B38**, 881 (1982).  
[15] V. M. Lynch, S. H. Simonsen, R. F. Miller, J. C. Turley and G. E. Martin, *ibid.*, **C41**, 1240 (1985).  
[16] A. S. Zektzer, G. E. Martin and R. N. Castle, *J. Heterocyclic Chem.*, **24**, 879 (1987).  
[17] A. S. Zektzer, L. D. Sims, R. N. Castle and G. E. Martin, *Magn. Reson. Chem.*, **26**, 287 (1988).  
[18] L. Müller, *J. Magn. Reson.*, **59**, 326 (1984).  
[19] J. Cavanagh and J. Keeler, *J. Magn. Reson.*, **7**, 612 (1988).  
[20] A. Bax, *J. Magn. Reson.*, **53**, 517 (1983).  
[21] M. S. Chauhan and I. W. J. Still, *Can. J. Chem.*, **53**, 2880 (1975).  
[22] A. S. Zektzer, B. K. John and G. E. Martin, *Magn. Reson. Chem.*, **25**, 752 (1987).  
[23] P. E. Riley and R. E. Davis, *Acta Cryst.*, **B32**, 381 (1976).  
[24] P. Main, S. E. Hull, G. Germain, L. E. Lessinger, J. P. Declercq and M. M. Woolfson, MULTAN78, A System of Computer Programs for the Automatic Solution of Crystal Structures from X-Ray Diffraction Data, Universities of York, England and Louvan, Belgium.  
[25] G. M. Sheldrick, SHELEX76. A Computer Program for Crystal Structure Determination, University of Cambridge, England.  
[26] D. T. Cromer and J. B. Mann, *Acta Cryst.*, **A24**, 321 (1968).  
[27] R. F. Stewart, E. R. Davidson and W. T. Simpson, *J. Phys. Chem.*, **42**, 3175 (1965).  
[28] International Tables for X-Ray Crystallography, Vol IV, Kynoch Press, Birmingham, 1974, p 55.  
[29] A. W. Cordes, personal communication (1983).  
[30] S. M. Gadol and R. E. Davis, *Organometallics*, **1**, 1607 (1982).